THE ASTROPHYSICAL JOURNAL, 484:810–819, 1997 August 1

ON THE RELATIVE IMPORTANCE OF PHOTOEVAPORATIVE AND HYDRODYNAMIC EFFECTS IN THE ABLATION OF SELF-GRAVITATING GLOBULES IN COMPACT H II REGIONS

S. J. ARTHUR AND S. LIZANO
Instituto de Astronomía, Universidad Nacional Autónoma de México, Apdo. Postal 70-264, 04510 México D.F., Mexico
Received 1996 November 15; accepted 1997 March 6

ABSTRACT

We investigate in detail the process of hydrodynamic ablation, both for the case of subsonic and for supersonic flows, of isothermal self-gravitating globules. The results are then compared with those for photoevaporative mass loss to estimate which of the two processes is the dominant mechanism for the mass loss of self-gravitating globules embedded in compact H II regions. This material then goes on to mass-load the stellar wind, thereby altering its dynamical properties. Using our results, we perform numerical simulations of the evolution of such H II regions, taking into account both possible mass-loading processes, together with the effect of the finite lifetime of the globules. We find that for compact H II regions with central stars possessing high ionizing photon rates the photoevaporation process dominates.

Subject headings: hydrodynamics — ISM: globules — ISM: H II regions — stars: mass loss

1. INTRODUCTION

Mass loading of stellar winds from young massive stars has been proposed as a mechanism to lengthen the compact phase of H II regions. Neutral globules, possibly remnants from the star formation process, act as reservoirs of gas inside the H II region, keeping the density inside the H II region high enough such that the Strömgren radius does not increase with time. This confinement process lasts for timescales $\sim 10^5$ yr, as long as the neutral globules survive (Dyson 1994; Lizano & Cantó 1995; Dyson, Williams, & Redman 1995; Redman, Williams, & Dyson 1996; Lizano et al. 1996, hereafter LCGH).

The fresh material from these globules can be injected into the ionized flow of the H II region by photoevaporation and hydrodynamic ablation. The rate of photoevaporation depends on the flux of ionizing photons that arrives at the surface of the neutral globule. Each Lyman continuum photon that reaches the surface of the globule liberates an electron/proton pair. This flux is much less than the stellar ionizing photon flux because of the absorption by dust and recombinations in the evaporating material (see, e.g., LCGH).

The process of hydrodynamic ablation of pressure-confined clumps was studied by Hartquist et al. (1986, hereafter HDPS). A dense clump exposed to a subsonic flow will expand in the direction perpendicular to the flow as a result of pressure imbalances set up around the body. Mixing of expanding clump material into the flow occurs when the expansion has gone on long enough so that the rate of mass flow through the mixing region is proportional to the clump mass-loss rate. HDPS showed that if the clump expands by means of an isothermal rarefaction wave, its mass-loss rate is proportional to the 4/3 power of the Mach number of the incident flow. In the case of a supersonic flow incident upon a pressure-confined clump, the mass loading was assumed to saturate at the value obtained by setting the Mach number equal to unity in the subsonic case. The effect of mass loading by hydrodynamic ablation of pressure-confined clumps in a variety of astrophysical flows, such as Wolf-Rayet ring nebulae, planetary nebulae, and supernova remnants, has also been studied (e.g., HDPS; Arthur, Dyson, & Hartquist 1993, 1994; Arthur & Henney 1996).

However, the neutral globules proposed as the mass source in compact H II regions are expected to be self-gravitating, in which case the analysis of HDPS is no longer valid. Murray et al. (1993) showed that a gravitational field stabilizes clouds embedded in winds against mass loss by this method. Neutral globules have been observed in the Orion region, where they are being evaporated. These globules are known to have stars in their centers and so must be self-gravitating (O'Dell, Wen, & Hu 1993; McCaughrean & Stauffer 1994; O'Dell & Wen 1994; Henney et al. 1996). Externally ionized globules (the so-called PIGs) have been observed in several compact H II regions (see, e.g., Laques & Vidal 1979; Felli, Hjellming, & Cesaroni 1987; Garay, Moran, & Reid 1987; Churchwell et al. 1987; Garay 1987; Felli et al. 1993). It is thought that these globules could be cores about to undergo collapse to form low-mass stars and hence would also be self-gravitating. The contour maps resulting from radio surveys of a number of irregular H II regions (Wood & Churchwell 1989; Kurtz, Churchwell, & Wood 1994) yield globule radii between 0.006 and 0.02 pc and a number density of globules of between 2×10^3 and 3×10^4 pc^{-3}. A typical radius is $R_g \sim 0.01$ pc, and this is the value we adopt in this work. We assume a standard globule number density $N_g \sim 2 \times 10^4$ pc^{-3}, which is consistent with the values quoted above. Following LCGH, we assume that the mass of an individual globule is about 1 $M_\odot$, implying a velocity dispersion of order 1 km s^{-1} if the globule is in virial equilibrium. Globules with these typical values will hereafter be referred to as "standard" globules.

In this work, we formulate the problem of hydrodynamic ablation of self-gravitating globules and use these results to evaluate the relative importance of mass loading by photoevaporation versus mass loading by hydrodynamic ablation of such globules on the dynamics of the stellar wind coming from a young massive star in the center of a compact H II region. In particular, in self-gravitating globules, we find that the mass ablation must occur through supersonic and

subsonic mixing layers that have a much lower efficiency than the mixing processes in the case of the pressure-confined globules discussed above. Because of this, in the high ionizing photon fields characteristic of massive young stars, the photoevaporative processes dominate, thereby determining the form of mass loading of the compact H II regions and the corresponding evolution of the globules themselves.

2. SUPERSONIC FLOW PAST A SELF-GRAVITATING GLOBULE

A supersonic flow incident upon a globule will produce the familiar bow shock ahead of the body and tail shocks downstream of it. The flow behind the bow shock will be subsonic at the head of the body and supersonic to a lesser or greater extent along the sides, depending on the angle between the shock and the incident flow. The shock angle at which the flow becomes supersonic is about 60° for incident Mach numbers greater than 2 (see, e.g., Landau & Lifschitz 1987). An examination of supersonic flow around solid spherical bodies (Van Dyke 1982) suggests that this angle corresponds to about 45° measured from the center line parallel to the flow direction. Thus the flow around the sides of the body is mainly supersonic, and one can expect a supersonic turbulent mixing layer to form between the gas of the flow and that of the self-gravitating globule (see, e.g., Fig. 1).

The gross properties of supersonic turbulent mixing layers have been discussed by Cantó & Raga (1991, hereafter CR). They considered the mixing layer between a plane, pressure-matched flow and a homogeneous environment, taken to be at rest. They assume that the flow, mixing layer, and environment are in pressure equilibrium and use quantities averaged across the layer to permit a single-parcel approach. For layers with small opening angles, the flow in the layer should be well approximated by a Couette flow. Under the above assumptions, the entrainment of mass from the flow and environment into the layer is investigated. The entrainment process is characterized by an efficiency factor, ϵ, and upper limits are derived for it from hydrodynamic considerations. In order to fix the value of ϵ, a comparison is made with laboratory mixing-layer experiments. These experiments correspond to approximately adiabatic flows, cover a range of Mach numbers from zero to 20 and have effectively infinite Reynolds numbers. Hence they are very applicable to astrophysical flows. The experimental results fix the constant of proportionality in the theoretical model, which yields an excellent fit to the laboratory data. Although laboratory data only exist for the adiabatic case, CR speculated that the value of ϵ will be valid, at least approximately, in the nonadiabatic case as well. Obviously, the case of nonadiabatic mixing layers requires further theoretical and experimental investigation, but in the absence of other work on the subject, we will suppose that the value of ϵ derived by CR holds for the nonadiabatic case.

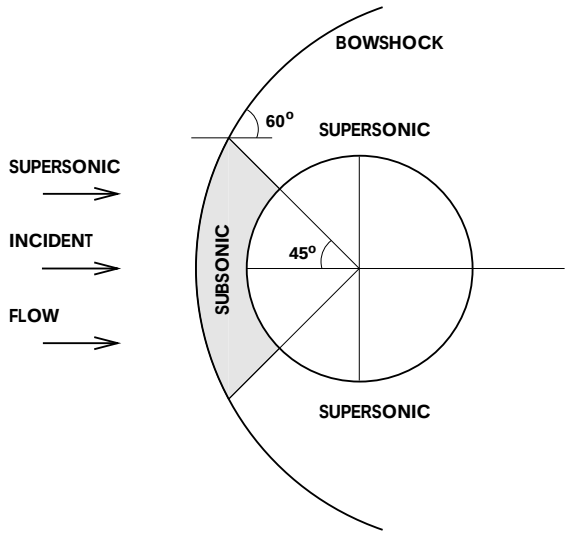

FIG. 1.—Subsonic and supersonic flow regions for flow around a sphere

The entrainment velocity of material from the environment (in this case the globule) into the flow cannot be greater than the sound speed in the environment material, c_0 (in this case, the isothermal sound speed in the self-gravitating globule), and thus the amount of material entrained in the layer from the globule per unit area is given by

$$\dot{\sigma} = \epsilon \rho_0 c_0 , \tag{1}$$

where ρ_0 is the density at the edge of the globule and ϵ is the entrainment efficiency factor, given by

$$\epsilon \simeq 0.09 \min\left(1, \frac{c_0}{2c_s}, \frac{c_0}{3c_L}\right). \tag{2}$$

In equation (2), c_s refers to the post–bow shock flow sound speed and c_L refers to the sound speed in the mixing layer itself. The three terms in parentheses refer respectively to the "globule limited," "flow limited," and "mixing-layer limited" regimes. CR conjectured that most astrophysical cases (e.g., the entrainment of environmental material by a stellar jet) fall into the third of these categories.

In this work we assume that the mixing layer is isothermal. Turbulent heating of the gas in the layer is followed by efficient radiative cooling of the dense mixing-layer gas to $\sim 10^4$ K (see, e.g., Taylor & Raga 1995). Hence the sound speed in the mixing layer is given by $c_L = c_i$, where c_i is the sound speed of ionized gas at 10^4 K.

In Appendix A, we show that for incident flow Mach numbers $M_w < 65$, the cooling time of the post–bow shock flow is smaller than the time it takes a parcel of gas to travel the length of the mixing layer (see Fig. 2). For this range of Mach numbers, the postshock flow can thus be considered isothermal, with $c_s = c_i$, where c_i is also the sound speed in the incident ionized flow. For higher incident Mach numbers, $M_w \geq 65$, the postshock sound speed will depend on the velocity of the incident flow, since the gas will not cool while traveling along the mixing layer. In this case, the sound speed is given approximately by $c_s \simeq u_w/2$, where u_w is the incident flow velocity (see eq. [A2]).

Hence, for $M_w < 65$ we have $c_s = c_i$ and $c_L = c_i$, and so equation (2) implies that we are indeed in the "mixing-layer limited" regime; thus we take $\epsilon = 0.09 c_0/(3c_i)$. For $M_w \geq 65$, however, we find $c_s = u_w/2 \gg c_i$, which indicates that we are in the "flow limited" regime and that $\epsilon = 0.09 c_0/u_w$. However, since the mass-loading process has the effect of lowering the wind velocity (and hence the Mach number), then for all but the innermost parts of the H II region (where the mass-loaded stellar wind velocity will be highest) we can assume that $c_s = c_i$.

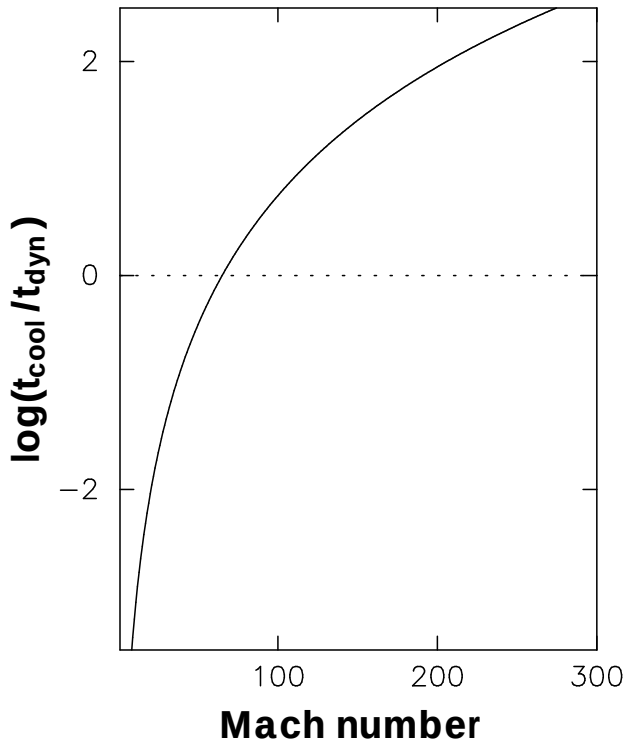

FIG. 2.—Ratio of cooling time to dynamic time vs. Mach number for post–bow shock flow.

It is clear from the above considerations that for most cases we can assume that we are in the "mixing-layer limited" regime. This yields an upper limit to the entrainment efficiency factor of $\epsilon = 0.09 c_0/(3c_i)$. The mass loss per unit area, $\dot{\sigma}$, to the layer from the globule is therefore given by

$$\dot{\sigma} = 0.09 \frac{\rho_0 c_0^2}{3c_i} . \tag{3}$$

If we suppose that the turbulent mixing layer extends from the sonic point at $\theta \simeq 45°$ around a quarter of the circumference of the body (turbulent boundary layers separate farther back on the body than laminar boundary layers; Van Dyke 1982), then the area of the mixing layer is $A_L = 2(2)^{1/2}\pi R_g^2$, where R_g is the radius of the globule.

The hydrodynamic mass ablation rate from the globule is given by $\dot{m}_{\rm hyd} = A_L \dot{\sigma}$. On substituting the density distribution of an isothermal self-gravitating sphere, $\rho_0 = c_0^2/(2\pi G R_g^2)$, where G is the gravitational constant, the total mass loss through the mixing layers of the globule is

$$\dot{m}_{\rm hyd} \simeq \frac{1}{24G} \frac{c_0^4}{c_i} . \tag{4}$$

The total mass ablation rate for the supersonic turbulent mixing layer of a self-gravitating globule is therefore independent of the incident flow velocity and density (cf. HDPS) and is also independent of the globule radius, R_g.

3. SUBSONIC FLOW PAST A SELF-GRAVITATING GLOBULE

In the case of non–self-gravitating, pressure-confined globules, subsonic flow around the globule leads to pressure gradients along the sides due to the Bernoulli effect. This pressure reduction leads to a lateral expansion of the globule via an isothermal rarefaction wave until the mass flux of the subsonic flow through the expansion region is equal to the mass flux of the expanding material and mixing can be said to occur (HDPS). In the case of self-gravitating globules this mechanism does not work, because the gravitational field of the clump prevents outflow and mass loss (Murray et al. 1993). If we suppose that the globule is initially in a stable configuration with a certain definite value of the central density, then if the self-gravity of the globule is large enough, fluctuations in the external pressure can be accommodated by the globule's adopting a different value for the central density (Bonnor 1956).

An alternative way of losing mass could be due to the fact that a subsonic flow arriving at the globule can be supersonic with respect to the globule gas, since the globules are cold. A shock wave will then be sent into the globule, which will heat the gas, and if the heating is sufficient, this shocked gas could acquire a thermal velocity great enough to leave the potential of the globule. Nevertheless, as shown in Appendix B, the shock propagating into the globule will be isothermal, and this process produces no mass loss.

3.1. *Subsonic Mixing Layers*

A subsonic flow past a globule will form a turbulent mixing layer in a similar way to the supersonic case discussed above. However, in this case the entrainment velocity of material into the mixing layer is not fixed by the sound speed of the globule material, but instead by the velocity of the dominant flow features in the mixing layer (Papamoschou & Roshko 1988). The entrainment process is governed by the large eddies in the turbulent mixing layer, and hence the entrainment velocity is given by the velocity of these large structures. Once entrained into the mixing layer, smaller scale mixing occurs across the main body of the mixing layer, and mean properties can then be defined. The velocity of the dominant structures, U_c, is known as the *convective* velocity. For flows with equal ratios of specific heats (i.e., equal γ; true in our case because both the incident ionized flow and the molecular globule gas are considered isothermal, for which $\gamma = 1$), U_c is given by

$$U_c = \frac{a_2 U_1 + a_1 U_2}{a_1 + a_2} , \tag{5}$$

where U_1 and U_2 are the undisturbed flow velocities in the two fluids and a_1 and a_2 are the respective sound speeds. Hence U_c is a sound-speed–weighted average. In this work, $a_1 = c_0$, $a_2 = c_i$, $U_1 = 0$, $U_2 = u_w$, and equation (5) becomes

$$U_c = \frac{c_0 u_w}{c_i + c_0} . \tag{6}$$

Since for an ionized H II region the sound speed in the ionized gas, c_i, is much greater than the sound speed in the molecular gas, c_0, we have

$$U_c \simeq c_0 M_w , \tag{7}$$

where $M_w = u_w/c_i$ is the Mach number in the (subsonic) wind.

Equation (7) only gives the entrainment velocity for Mach numbers $M_w \leq 1$, because the entrainment velocity, given by U_c, cannot be greater than the sound speed in the globule, c_0.

The mass per unit area entrained from the globule by the turbulent layer is given by

$$\dot{\sigma} = \epsilon^* \rho_0 c_0 M_w , \tag{8}$$

where ϵ^* is the entrainment efficiency, which in this case should reflect the intermittent nature of the large eddies.

We now consider the subsonic and supersonic flow regions generated by the flow of a subsonic stream around a rigid sphere. For flow Mach numbers of about 0.4, the flow around the sphere becomes supersonic at the point where the flow is tangential to the globule's surface, although the extent of the supersonic region is very small (see, e.g., Botta 1995). As the incident flow Mach number increases, so does the size of the supersonic flow region. Thus the evaluation of A_L, the area of the mixing layer, becomes rather complicated. In order to simplify matters we will take the same value of A_L as was used in the supersonic mixing layer case.

We also require that the subsonic and supersonic mixing layer solutions match for flow Mach numbers $M_w = 1$. For this reason, we adopt the same entrainment efficiency parameter as in the supersonic mixing layer case, that is, $\epsilon^* = \epsilon = 0.09 c_0/(3c_i)$, as above.

The total mass ablation rate, $\dot{m}_{\rm hyd} = A_L \dot{\sigma}$, is then

$$\dot{m}_{\rm hyd} \simeq \frac{1}{24G} \frac{c_0^4}{c_i} M_w . \tag{9}$$

This equation should be compared with equation (4). Hence, in the subsonic case the ablation (or entrainment) rate is proportional to the Mach number of the incident flow, whereas in the supersonic case it is independent of it for $M_w < 65$. This result can be compared to that of HDPS, who found that for non–self-gravitating globules the ablation rate was proportional to $M_w^{4/3}$ for the subsonic case and assumed independent of the flow Mach number in the supersonic case.

4. COMPARISON WITH PHOTOEVAPORATIVE MASS LOSS

Now that we have a picture of the processes of hydrodynamic ablation that one might expect from self-gravitating globules in a stellar wind, we want to compare it with mass loss by photoevaporation, as discussed by LCGH. We first assume that both processes can occur at the same time in the same globule. This assumption comes from the observation that the hydrodynamic ablation processes are mixing-layer processes and essentially occur on the sides of the globules, where the photoevaporation is least effective. Dyson (1994) suggested that photoevaporation is suppressed when the ram pressure of the impacting stellar wind is greater than the pressure of the evaporating flow. This argument leads to the result that photoevaporative mass loss is most important in the outer regions of H II regions, where geometric dilution means that the ram pressure of the stellar wind becomes lower than that of the photoevaporating flow. However, this is a rather one-dimensional argument, and it could be expected instead that the photoevaporated material is swept back around the globule by the incident wind, such as has been postulated in the case of the proplyds, discussed by Henney et al. (1996), and, indeed, as occurs in bow shocks in general. Thus there is no ram pressure balance apart from at the stagnation point.

As in the ablation process, we consider that the photoevaporated material is mixed with the post–bow shock flow around the globule and accelerated up to the mean flow speed. In particular, for a D-critical ionization front the photoevaporated material leaves the ionization front with velocity c_i, the sound speed of the ionized gas. The flux of photoevaporated material from the ionizing front is then given by $n_{i,0} c_i = F_g$, where $n_{i,0}$ is the number density of the material leaving the ionization front and F_g is the flux of ionizing photons that arrives at the surface of the neutral globule. This flux yields the following implicit equation for $n_{i,0}$:

$$F_g = F_* e^{-(\tau_w + \tau_0)} - f(\tau_0) n_{i,0}^2 \alpha_B R_g , \tag{10}$$

where $F_* = \dot{S}/(4\pi d^2)$ is the stellar ionizing photon flux, $\dot{S}$ is the stellar ionizing photon rate, d is the distance of the globule from the star, τ_w and τ_0 are the dust extinction optical depths from the stellar wind and the globule photoevaporated material, respectively, and $\alpha_B = 2.6 \times 10^{-13}$ cm^{-3} s^{-1} is the case B recombination rate. In particular, for a density profile of evaporating material $n = n_{i,0}(r/R_g)^{-2}$, we have

$$f(\tau_0) = \tau_0^{-3}[\tau_0^2 - 2\tau_0 + 2(1 - e^{-\tau_0})] , \tag{11}$$

as described in Henney et al. (1996). Finally, $\tau_0 = \sigma_d n_{i,0} R_g$, where σ_d is the dust extinction cross section. The second term of equation (10) corresponds to the recombinations in the photoevaporated material, which in equilibrium are equal to the absorbed ionizing photons. Therefore, the photoevaporation rate of a globule is given by

$$\dot{m}_{\rm ph} = F_g(\pi R_g^2) m_{\rm H} = \pi R_g^2 n_{i,0} c_i m_{\rm H} , \tag{12}$$

where $m_{\rm H}$ is the proton mass.

The maximum hydrodynamic ablation rate occurs for incident wind Mach numbers $1 \le M_w \le 65$ (eq. [4]), while the photoevaporative mass-loss rate is given by equation (12). To facilitate a comparison between the two rates, we consider the dust-free case, for which $\sigma_d = 0$ and recombination terms will dominate. Hence, equation (10) yields

$$n_{i,0} = \left(\frac{3\dot{S}}{4\pi \alpha_B d^2 R_g} \right)^{1/2} . \tag{13}$$

For sound speed $c_i = 13$ km s^{-1} in the ionized gas, the ratio of ablation mass-loss rate to photoevaporative mass-loss rate is

$$\frac{\dot{m}_{\rm hyd}}{\dot{m}_{\rm ph}} \simeq 1.3 \frac{c_{0,1}^4 d_{\rm pc}}{\dot{S}_{49}^{1/2} R_{g,1}^{3/2}} , \tag{14}$$

where $c_{0,1}$ is the sound speed in the molecular globule gas measured in units of km s^{-1}, $d_{\rm pc}$ is the distance of the globule from the star expressed in units of 1 pc, $\dot{S}_{49}$ is the ionizing photon rate expressed in units of 10^{49} s^{-1}, and $R_{g,1}$ is the globule radius in units of 0.01 pc. Note that the values $c_{0,1}$ and $R_{g,1}$ correspond to those expected for "standard" globules in compact H II regions, mentioned in § 1. Equation (14) suggests that photoevaporation dominates in compact H II regions with small radii and high ionizing photon rates. In any case, hydrodynamic ablation will dominate close to the Strömgren radius, where the ionizing photon rate goes to zero. We can also see from equation (14) that as the globule size R_g decreases, hydrodynamic ablation becomes more important. This decrease is expected in the central part of the H II region, where the globules are destroyed at early times by photoevaporation. It can be seen from the above equation that the relative importance of hydrodynamic ablation increases if the sound speed in the globules increases. A higher globule sound

speed would mean either more massive or turbulent globules (if the globule radius remains fixed) or smaller globules (if the mass is fixed) with respect to the "standard" globules mentioned above.

5. RESULTS

In this section, we present the results of time-dependent calculations in which we investigate the effect on a stellar wind of the two mass-loading processes of photoevaporation and hydrodynamic ablation of embedded clumps as discussed in the previous sections. We consider "standard" globules, with radii $R_g = 0.01$ pc, gas sound speed $c_0 = 1$ km s^{-1}, and globule number density $N_g = 2 \times 10^4$ pc^{-3}. Such globules are representative of the PIGs that have been observed in compact H II regions (see § 1).

We follow the work of LCGH for the case of photoevaporated flows. We use the same equations for the ionizing photon rate, $\dot{S}$, and the density of material leaving the ionization front moving into the globule, $n_{i,0}$, and the usual isothermal gasdynamic equations for the mass-loaded wind density and velocity. We include the injection velocity of the photoevaporative material, which has a direction opposite to that of the flow and speed equal to the sound speed in the ionized gas (since a D-critical ionization front is assumed).

To facilitate comparison between the results of the present paper and LCGH, we adopt the same nondimensionalization. That is, distances are measured in units of $r_0 = (A_{g,0} N_g)^{-1}$, where $A_{g,0} = \pi R_{g,0}^2$ is the initial globule area facing the star and N_g is the number density of globules. This length is the mean free path for a photon to hit a globule. Velocities, u, are measured in units of the ionized sound speed, c_i; densities, ρ, in units of $\rho_0 = m_H[\dot{S}_*/(4\pi r_0^3 \alpha_B)]^{1/2}$; mass-loading rate, $\dot{m}$, in units of $\dot{m}_0 = \rho_0 c_i A_{g,0} N_g$; and ionizing photon rate, $\dot{S}$, in units of $\dot{S}_*$, the ionizing photon rate at the star.

As an illustrative example we consider the case of an O6 star, with a stellar wind mass-loss rate of $10^{-6}\ M_\odot$ yr^{-1}, wind terminal velocity of 2800 km s^{-1}, and flux of ionizing photons of 1.2×10^{49} s^{-1}. The photoevaporative mass-loss rate depends on the size of the globules as described in equation (12), whereas the mass loss by hydrodynamic ablation is independent of the globule size and only depends on the Mach number of the incident flow as given by equations (4) and (9). Our calculations assume that the globules are embedded in a preexisting, steady state stellar wind and that the ionizing photons are instantaneously switched on at time $t = 0$. Prior to this moment we consider no photoevaporation or hydrodynamic ablation of the globules. This initial condition ignores the effect of hydrodynamic ablation of the globules on the stellar wind while the initial steady state wind is being established. It also assumes that the wind is set up before the ionizing photons are switched on. Since the setting up of a steady state wind plus ionizing photon flux is a complex problem (e.g., initially the stellar wind and photon flux will be variable), the above initial conditions are adopted for simplicity. In any case, a posteriori, we find that the hydrodynamic ablation rate is very small and does not have a significant effect on the stellar wind at the small radii important for compact H II regions. Had the hydrodynamic ablation rate been more significant, the initial condition would have had to take this into account.

As soon as the ionizing photons are switched on, both photoevaporation and hydrodynamic ablation are included in the calculation, leading to mass loading of the stellar wind and erosion of the globules. The mass of the globule, M_g, decreases with time according to

$$\frac{\partial M_g}{\partial t} = -(\dot{m}_{\rm ph} + \dot{m}_{\rm hyd}) \,. \tag{15}$$

Assuming that the globules are virialized with constant velocity dispersion, the decrease in the globule radius can be found from

$$\frac{M_g(t)}{R_g(t)} = \frac{M_{g,0}}{R_{g,0}} \,, \tag{16}$$

where $M_{g,0}$ and $R_{g,0}$ are respectively the globule mass and radius at time $t = 0$, when the mass-loss processes begin. The photoevaporation rate diminishes with the size of the globules, and so the importance of hydrodynamic ablation grows with time.

This calculation differs from that of LCGH in that they assumed that a steady state of a mass-loaded stellar wind was set up before the globules began to decrease in size. In the current paper, no such initial steady state is postulated. Furthermore, the calculation assumes that the gas is isothermal throughout the numerical grid. This is certainly true in regions where there is a high flux of ionizing photons, but close to the recombination front, and definitely beyond it, this assumption breaks down and our solution is no longer valid. For this reason, all the results shown stop at the radius of the recombination front, since an adiabatic treatment of the flow should really be considered thereafter. We note that since the recombination front coincides with the sonic point for all but early times of the evolution, the flow beyond the recombination front cannot affect that inside it, and so our results up to this point will not be affected by the adiabatic part of the flow.

In Figure 3, we show how the mass-loading rates due to both photoevaporation and hydrodynamic ablation change with evolution of the H II region. In the case of photoevaporation, we show the photoevaporative mass-loss rate at three times, $t = 10^3$, 10^4, and 10^5 yr. The hydrodynamic mass-loss rate is only shown for $t = 10^5$ yr because it does not change appreciably. We see that for the entire H II region up to the recombination front the photoevaporation dominates. Only at late times, when the innermost globules have been almost completely evaporated, do the photoevaporative and hydrodynamic ablation mass-loss rates become comparable. A comparison of Figure 3 with Figure 3 of LCGH shows how the two calculations differ. In the present work, the photoevaporation rate has a "knee" at the isothermal shock front at early times, then tails off toward the sonic point. This is because the density of the mass-loaded stellar wind jumps sharply after the shock, and so more of the ionizing photons are absorbed; hence the mass-loading due to photoevaporation falls. In the work of LCGH, for simplicity, a constant $\dot{S}$ was assumed for the calculation of $\dot{q}(r, t)$ in their Figure 3, and hence their $\dot{q}$ is a continuous smooth curve [however, their models do take into account $\dot{S}(r)$ for the remaining calculations].

In Figure 4, we plot the ratio of photoevaporative to hydrodynamic mass-loading rate for the times $t = 10^4$ and 10^5 yr for three stars, O6, O9, and B0, whose properties are listed in Table 1 of LCGH. In each case the peak in the ratio occurs just after the isothermal shock, when the mass-loaded wind has gone subsonic and the hydrodynamic

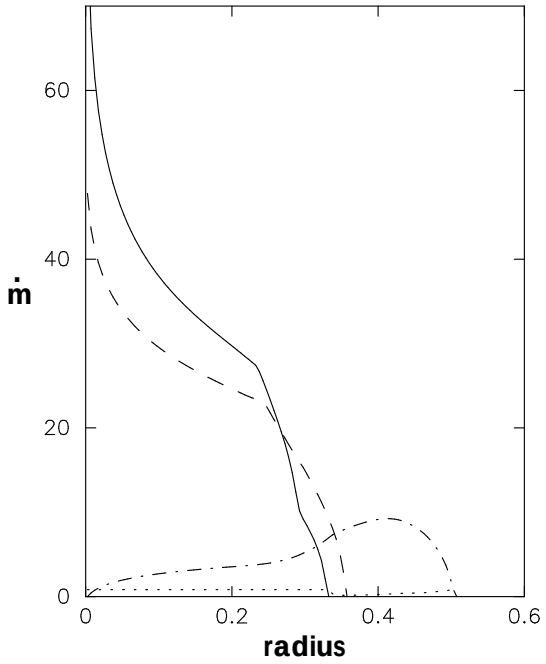

FIG. 3.—Mass-loading rate vs. radius. Photoevaporative mass loss: $t = 10^3$ yr (*solid line*), 10^4 yr (*dashed line*), and 10^5 yr (*dot-dashed line*). Hydrodynamic ablation: $t = 10^5$ yr (*dotted line*). All quantities are nondimensionalized as described in § 5.

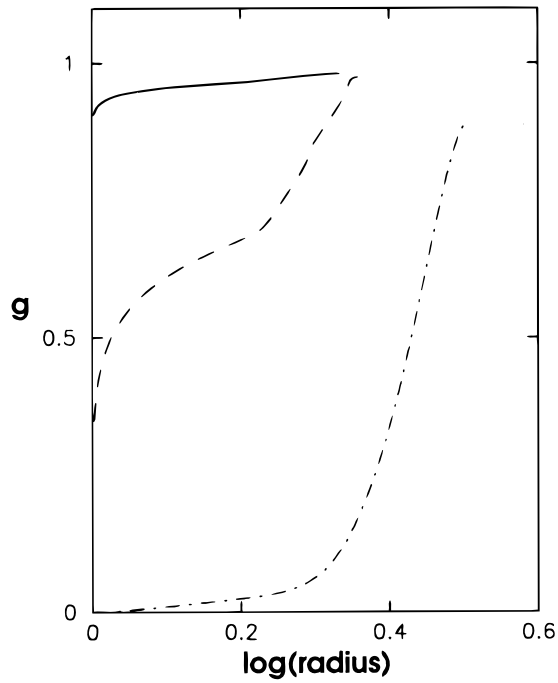

FIG. 5.—Globule area function vs. radius. The line styles refer to the same times as in Fig. 3. Radius is given in nondimensional units as described in § 5.

mass-loading rate is a minimum. It can be seen in each case that the photoevaporation decreases in the center as the evolution proceeds and the innermost globules are completely evaporated.

Figure 5 shows how the globule radius, $R_g = R_{g,0} g^{1/2}$, changes with time, where g is the nondimensional area function and $R_{g,0}$ is the initial globule radius, as described by LCGH in their § 2.3. As expected, it is the innermost globules that are evaporated first. In Figure 6, the number of ionizing photons versus radius is displayed. We note how between 10^3 and 10^4 yr the position of the recombination front does not change much with time while, by 10^5 yr, it has started to move outward, as there is not enough ablated

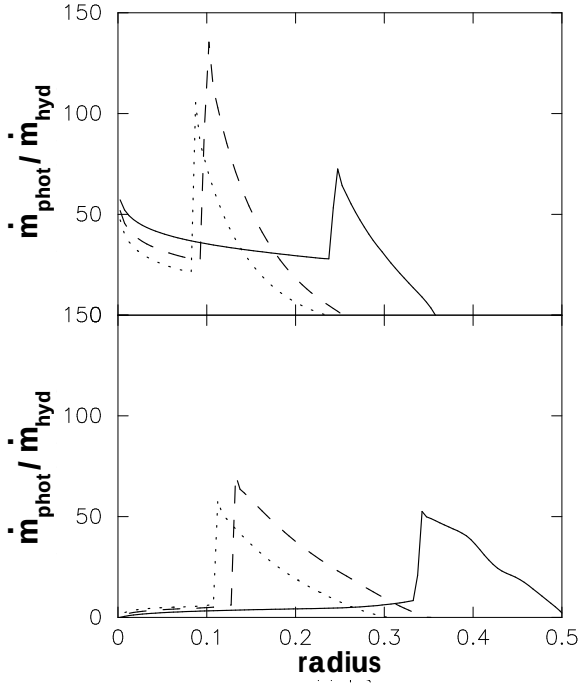

FIG. 4.—Ratio of photoevaporative to hydrodynamic mass-loading rates vs. radius. *Top*, $t = 10^4$ yr; *bottom*, $t = 10^5$ yr. *Solid line*, O6 star; *dashed line*, O9 star; *dotted line*, B0 star. Parameters for these stars are given in Table 1 of LCGH. Radius is given in nondimensional units as described in § 5.

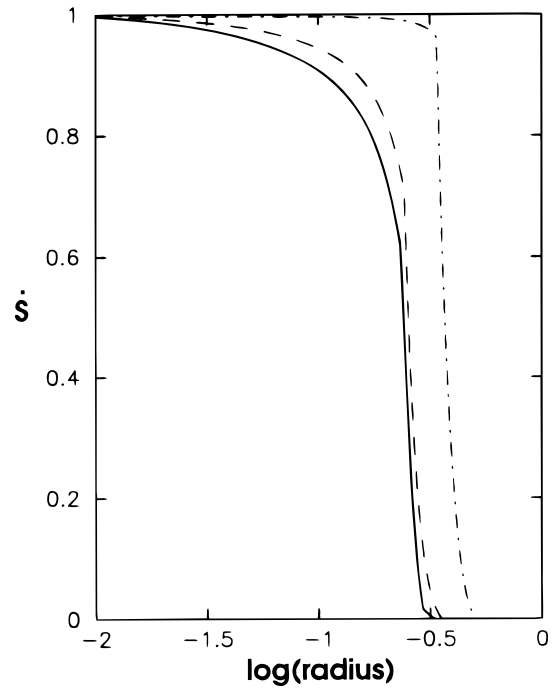

FIG. 6.—Ionizing photon rate vs. radius. The line styles refer to the same times as in Fig. 3. All quantities are nondimensionalized as described in § 5.

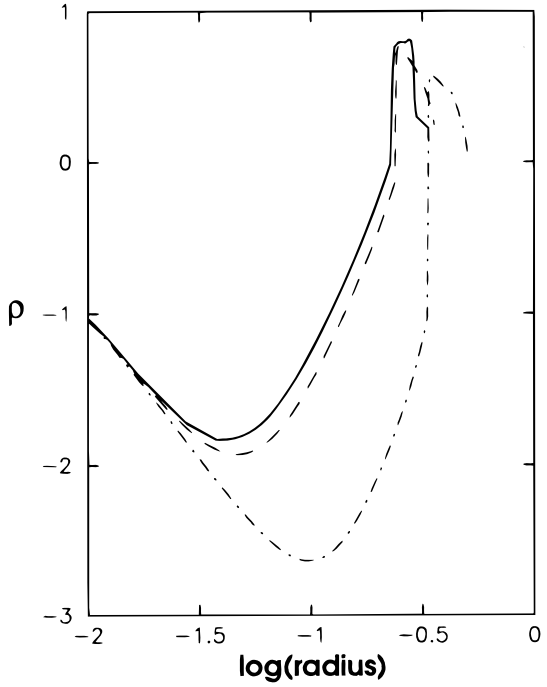

FIG. 7.—Gas density (stellar wind plus mass-loaded material) vs. radius. The line styles refer to the same times as in Fig. 3. All quantities are nondimensionalized as described in § 5.

material in the inner regions of the H II region to maintain it in a fixed position. Further, as the density in the inner part of the H II region drops with time, most of the photons reach the zone of the shock and recombination front, leading to a flatter profile for the number of ionizing photons as a function of radius.

Figures 7 and 8 show how the density and velocity respectively change with radius at the same times given above. We see that a shock wave forms interior to the recombination front, and, like the sonic point, its position is steady at early times. However, this shock wave strengthens with time and then starts to move outward once the globule material in the inner regions becomes used up. Thus the mass-loading process is unable to confine the Strömgren radius for times longer than $\sim 10^5$ yr.

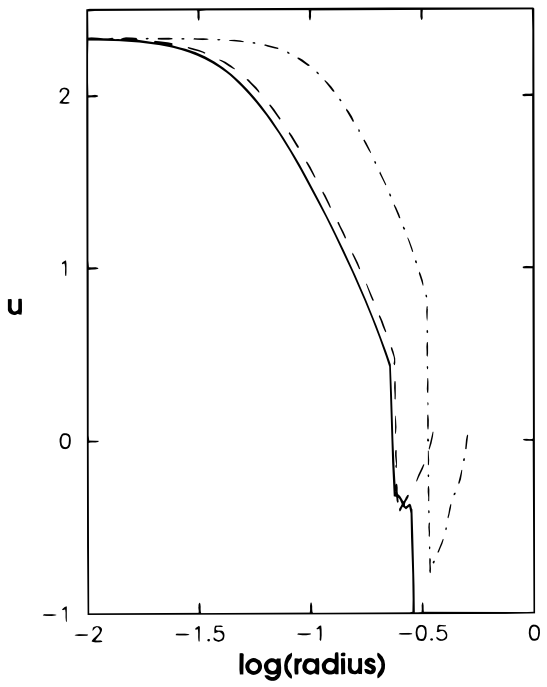

FIG. 8.—Velocity vs. radius. The line styles refer to the same times as in Fig. 3. All quantities are nondimensionalized as described in § 5.

6. CONCLUSION

We have shown, by detailed calculation, that hydrodynamic ablation of self-gravitating globules immersed in compact H II regions around massive stars possessing stellar winds can only take place in mixing layers around the sides of the globules. For the case of subsonic flow, the mass-loss rate is proportional to the Mach number of the flow, while in the supersonic case the ablation rate saturates and is a constant for Mach numbers $M_w < 65$. For higher Mach numbers, $M_w > 65$, the mass-loss rate is proportional to the wind speed.

We have shown that for such globules photoevaporation is the dominant mass-loss mechanism, initially exceeding the hydrodynamic ablation rate by almost 2 orders of magnitude in the inner parts of the H II region. Only at late times ($t \sim 10^5$ yr) do the two processes become competitive. This is because the photoevaporation rate is proportional to the area of the face of the globule that is ionized by the central star, πR_g^2, and hence decreases as the globule size decreases. On the other hand, the hydrodynamic ablation rate is independent of the globule size. In particular, hydrodynamic ablation can become important in the central regions, where the globules photoevaporate faster, and at the Strömgren radius, where the ionizing photon rate $\dot{S}$ drops to zero. The hydrodynamic ablation rate depends on the physics of the mixing-layer process, as discussed in § 2. The efficiency of the entrainment process has been quantified by comparison with the results of laboratory experiments (CR). The actual value of this efficiency may differ since the flows discussed in this paper are assumed to be isothermal, whereas the laboratory experiments are adiabatic. The potential change is insignificant in comparison with the 2 orders of magnitude we find separating photoevaporative and hydrodynamic mass loss and so would not change our conclusions.

Our results show that globules with the characteristics of our "standard" globules are depleted faster in the innermost parts of the H II region but still last some 10^5 yr (see also LCGH). After this time the size of the region steadily grows, as there is insufficient ablated material to maintain the recombination front in a fixed position. Nevertheless, the survival timescales of the globules are long enough to make the mass loading of stellar winds a promising mechanism to lengthen the compact phase of H II regions and therefore explain the high observed numbers of such regions (Wood & Churchwell 1989).

As found by LCGH, the recombined neutral flow leaving the H II region should be transonic and, in principle, can be calculated by using the values of the hydrodynamic variables at the recombination front as boundary conditions for the adiabatic flow.

The authors would like to acknowledge financial support from DGAPA, Universidad Nacional Autónoma de México, through project IN102395 and from CONACYT through grant 4916-E9406. We thank Will Henney and Alex Raga for useful discussions.

APPENDIX A

COOLING TIME OF THE POST–BOW SHOCK FLOW

In this appendix, we investigate the cooling of the gas that has passed through the bow shock that forms ahead of a globule when the incident flow is supersonic. We assume that the post–bow shock flow is adiabatic and proceed to calculate its temperature and cooling time.

The temperature behind an oblique shock is given by

$$T_2 = T_1 \frac{\gamma - 1}{(\gamma + 1)^2} \left(2\gamma M_1^2 \sin^2 \phi - \frac{\gamma^2 - 6\gamma + 1}{\gamma - 1} - \frac{2}{M_1^2 \sin^2 \phi} \right), \tag{A1}$$

where M_1 and T_1 are the preshock Mach number and temperature, respectively, ϕ is the angle between the shock and the incident flow, and γ is the ratio of specific heats. The highest temperature possible in the supersonic post–bow shock flow is that for the critical angle $\sin \phi \simeq 3^{1/2}/2$. For this angle, and using $\gamma = 5/3$, we find

$$T_2 = \frac{T_1}{64} \left(15M_1^2 + 56 - \frac{16}{M_1^2} \right). \tag{A2}$$

Supposing that the incident flow is ionized, with a temperature $T_1 \simeq 10^4$ K, then the postshock temperature ranges $10^4 \text{ K} \leq T_2 \leq 10^5$ K and $10^5 \text{ K} < T_2 \leq 5 \times 10^7$ K correspond to incident Mach number ranges $1 \leq M_1 \leq 6.24$ and $6.24 < M_1 \leq 146$. The cooling time of the postshock gas can be estimated by assuming simple power laws for the cooling function (with units ergs $\text{cm}^{-3}\ \text{s}^{-1}$) in these temperature ranges of the form

$$L = n^2 \Lambda(T) , \tag{A3}$$

where n is the number density and $\Lambda(T)$ is a function of temperature of the form

$$\Lambda(T) = a_i T^{\beta_i} , \tag{A4}$$

where the subscript i refers to the two temperature ranges specified above. The a_i and β_i are constants depending on the temperature range (Arthur et al. 1993), such that

$$a_i = \begin{cases} 1.19 \times 10^{-27} , & \text{if } 10^4 \text{ K} \leq T \leq 10^5 \text{ K} \quad (i = 1) , \\ 1.19 \times 10^{-19} , & \text{if } 10^5 \text{ K} < T \leq 5 \times 10^7 \text{ K} \quad (i = 2) , \end{cases} \qquad \beta_i = \begin{cases} 1.1 , & \text{if } i = 1 , \\ -0.5 , & \text{if } i = 2 . \end{cases} \tag{A5}$$

The cooling time is given by

$$t_{\text{cool}} = \frac{p_2}{(\gamma - 1)L} , \tag{A6}$$

where p_2 is the postshock gas pressure.

Using equations (A1) and (A3), we can write equation (A6) in the following way:

$$t_{\text{cool}} = \frac{3k}{2a_i} \frac{T_1^{1-\beta_i}}{n_1} \frac{(15M_1^4 + 56M_1^2 - 16)^{1-\beta_i}(4 + M_1^2)}{4^{4-3\beta_i} M_1^{4-2\beta_i}} , \tag{A7}$$

where k is Boltzmann's constant and n_1 is the preshock number density of the incident flow.

These cooling times should be compared with the time taken for a parcel of gas to traverse the mixing layer, given by $t_{\text{dyn}} = X/v_2$, where $X = \pi R_g/2$ is the length of the mixing layer and v_2 is the postshock velocity, given by

$$v_2 = \frac{c_i}{8M_1} (48 + 24M_1^2 + 19M_1^4)^{1/2} \tag{A8}$$

for the parameters adopted above, where c_i is the sound speed in the incident flow. It can be seen from Figure 2 that for estimated values $n_1 \simeq 10^4\ \text{cm}^{-3}$ and $R_g \simeq 0.01$ pc pertinent to a compact H II region, then $t_{\text{dyn}} \geq t_{\text{cool}}$ for Mach numbers $M < 65$, and hence the post–bow shock flow will cool quickly and can be treated as isothermal, i.e., $c_s = c_i$. For higher Mach numbers, the post–bow shock sound speed varies approximately as $c_s \simeq u_w/2$, and the flow cannot be considered isothermal.

APPENDIX B

MASS LOSS DUE TO SHOCK HEATING OF GLOBULE MATERIAL

If we assume that the globules are cold, then a subsonic flow arriving at the globule can be supersonic with respect to the globule gas. A shock wave will then be sent into the globule, which will heat the gas, and if the heating is sufficient, this shocked gas could acquire a thermal velocity great enough to leave the potential well of the globule.

If we consider shock conditions along the globule axis for this case, then

$$\frac{p_2}{p_1} = 1 + \frac{2\gamma}{\gamma + 1}(M_1^2 - 1)\,, \tag{B1}$$

where subscript "2" denotes postshock properties, subscript "1" denotes preshock, or undisturbed, gas properties, p is pressure, and $M_1 = -U_s/c_0$ is the Mach number of the preshock gas in the shock frame, where U_s is the shock speed and c_0 is the sound speed in the undisturbed globule.

The postshock pressure must equal the subsonic flow pressure, given by the stagnation pressure, P_T, for flow along the globule axis. The preshock pressure is found from the pressure distribution in an isothermal self-gravitating globule, under the supposition that it acquires the limiting r^{-2} form

$$p_1 = p_I(r_I/r_s)^2\,, \tag{B2}$$

where r_s is the radius of the shock, measured from the globule center, and p_I is the pressure at some reference radius r_I. Rearranging equation (B1) and with the definitions $\mathscr{P} = P_T/p_I$ and $x = r_s/r_I$, we find

$$U_s = c_0\left[(\mathscr{P}x^2 - 1)\frac{\gamma + 1}{2\gamma} + 1\right]^{1/2}\,, \tag{B3}$$

whence

$$x = \left(\frac{\gamma + 1}{\gamma - 1}\mathscr{P}\right)^{-1/2} \sinh\left[\sinh^{-1}\left(\frac{\gamma + 1}{\gamma - 1}\mathscr{P}\right)^{1/2} - \frac{c_0}{r_I}\left(\frac{\gamma + 1}{2\gamma}\mathscr{P}\right)^{1/2} t\right], \tag{B4}$$

since

$$U_s = -r_I\frac{dx}{dt}\,. \tag{B5}$$

The shock velocity as a function of time is then given by

$$U_s = c_0\left(\frac{\gamma - 1}{2\gamma}\right)^{1/2} \cosh\left[\sinh^{-1}\left(\frac{\gamma + 1}{\gamma - 1}\mathscr{P}\right)^{1/2} - \frac{c_0}{r_I}\left(\frac{\gamma + 1}{2\gamma}\mathscr{P}\right)^{1/2} t\right]. \tag{B6}$$

We require that the postshock sound speed, c_2, be greater than the escape speed from the globule in order that thermal motions can lead to the shocked gas escaping from the globule's potential. That is, we require

$$c_2 \geq 2c_0\,, \tag{B7}$$

where

$$c_2^2 = \gamma\mathscr{P}x^2c_0^2\left[\frac{(\gamma - 1)\mathscr{P}x^2 + (\gamma + 1)}{(\gamma + 1)\mathscr{P}x^2 + (\gamma - 1)}\right]. \tag{B8}$$

Hence, for $\gamma = 7/5$ (assuming a molecular gas), equation (B7) is satisfied when

$$\mathscr{P}x^2 \gtrsim 12\,. \tag{B9}$$

This condition is valid for shock propagation times

$$0 \leq t \leq \frac{r_I}{c_0}\left(\frac{5}{4\mathscr{P}}\right)^{1/2}(\sinh^{-1} 2\sqrt{\mathscr{P}} - \sinh^{-1} 2\sqrt{12})\,. \tag{B10}$$

However, we also need to take into account the fact that the postshock material can cool. The temperature of the material behind the shock, T_2, is given by

$$T_2 = \left(\frac{\mu m_{\rm H} c_0^2}{k}\right)\mathscr{P}x^2\left(\frac{\mathscr{P}x^2 + 6}{6\mathscr{P}x^2 + 1}\right), \tag{B11}$$

where $\mu m_{\rm H}$ is the mean particle mass, k is Boltzmann's constant, and we have set $\gamma = 7/5$. Substituting reasonable numbers, and with the proviso given by equation (B9), we find

$$T_2 \gtrsim 346\mu \simeq 806\ {\rm K}\,, \tag{B12}$$

where we have supposed $c_0 = 1\ {\rm km\ s^{-1}}$. We also have the restriction that $T_2 < 10^4$ K, since at this temperature the globule gas would be ionized by the shock and cooling will be rapid. This restriction corresponds, for the same parameters as used above, to $\mathscr{P}x^2 < 207$.

For the temperature range considered, the cooling function can be crudely approximated by the constant value $\Lambda(T) = 10^{-25.5}$, where we have supposed an ionization fraction $\simeq 10^{-4}$ (Spitzer 1978). With this cooling law, we can estimate the cooling times of gas behind the shock traveling into the globule by using equations (A6) and (B11). Assuming that $\mu = 2.33$

in the globule gas, we obtain

$$t_{\rm cool} \simeq \frac{0.12}{\mathscr{P} p_I} (\mathscr{P} x^2)^2 \left(\frac{\mathscr{P} x^2 + 6}{6\mathscr{P} x^2 + 1} \right)^2 , \tag{B13}$$

where we recall that p_I is the reference pressure of the globule at radius r_I. For an isothermal self-gravitating globule, we have

$$p_I = \frac{c_0^4}{2\pi G r_I^2} , \tag{B14}$$

where $r_I = 0.01$ pc is now defined as the initial globule radius. For the allowed temperature range and corresponding values $12 \leq \mathscr{P} < 207$, we find that the cooling times fall within the range

$$0.011 \text{ yr} \leq t_{\rm cool} \leq 0.093 \text{ yr} , \tag{B15}$$

which is a consequence of the high pressure, and therefore density, in the outer regions of the globule. This high surface pressure demands a correspondingly high pressure in the surrounding compact H II region, which, in turn, results in a high density of ionized gas ($n_{\rm ion} \geq 10^4$ cm^{-3}). These cooling times are extremely short compared with the timescale for the shocked gas to escape from the globule potential,

$$t_{\rm esc} \simeq R_g / c_2 \simeq 10^4 \text{ yr} . \tag{B16}$$

Hence we conclude that the shock propagating into the globule must be isothermal for the physical conditions adopted in this work, and thus there can be no loss of material from the globule by this process.

REFERENCES

Arthur, S. J., Dyson, J. E., & Hartquist, T. W. 1993, MNRAS, 261, 425
———. 1994, MNRAS, 269, 1117
Arthur, S. J., & Henney, W. J. 1996, ApJ, 457, 752
Bonnor, W. B. 1956, MNRAS, 116, 351
Botta, N. 1995, J. Fluid Mech., 301, 205
Cantó, J., & Raga, A. C. 1991, ApJ, 372, 646 (CR)
Churchwell, E., Felli, M., Wood, D. O. S., & Massi, M. 1987, ApJ, 321, 516
Dyson, J. E. D. 1994, in Lecture Notes in Physics, 431, Star Formation Techniques in Infrared and mm-Wave Astronomy, ed. T. P. Ray & S. V. W. Beckwith (Berlin: Springer), 93
Dyson, J. E. D., Williams, R. J. R., & Redman, M. 1995, MNRAS, 277, 700
Felli, M., Churchwell, E., Wilson, T. L., & Taylor, G. B. 1993, A&AS, 98, 137
Felli, M., Hjellming, R. M., & Cesaroni, R. 1987, A&A, 182, 313
Garay, G. 1987, Rev. Mexicana Astron. Astrofis., 14, 489
Garay, G., Moran, J. M., & Reid, M. J. 1987, ApJ, 314, 535
Hartquist, T. W., Dyson, J. E., Pettini, M., & Smith, L. J. 1986, MNRAS, 221, 715 (HDPS)
Henney, W., Raga, A. C., Lizano, S., & Curiel, S. 1996, ApJ, 465, 216
Kurtz, S., Churchwell, E., & Wood, D. O. S. 1994, ApJS, 91, 659
Laques, P., & Vidal, J. L. 1979, A&A, 73, 97
Landau, L. D., & Lifschitz, E. M. 1987, Fluid Mechanics (2d ed.; Oxford: Pergamon)
Lizano, S., & Cantó, J. 1995, in Circumstellar Disks, Outflows and Star Formation, ed. S. Lizano & J. M. Torrelles (Rev. Mexicana Astron. Astrofis. Ser. Conf., 1) (México D.F.: Inst. Astron., Univ. Nac. Autónoma México), 29
Lizano, S., Cantó, J., Garay, G., & Hollenbach, D. 1996, ApJ, 468, 739 (LCGH)
McCaughrean, M. J., & Stauffer, J. R. 1994, AJ, 108, 1382
Murray, S. D., White, S. D. M., Blondin, J. M., & Lin, D. N. C. 1993, ApJ, 407, 588
O'Dell, C. R., & Wen, Z. 1994, ApJ, 436, 194
O'Dell, C. R., Wen, Z., & Hu, X. 1993, ApJ, 410, 696
Papamoschou, D., & Roshko, A. 1988, J. Fluid Mech., 197, 453
Redman, M., Williams, R. J. R., & Dyson, J. E. 1996, MNRAS, 280, 661
Spitzer, L., Jr. 1978, Physical Processes in the Interstellar Medium (New York: Wiley)
Taylor, S. D., & Raga, A. C. 1995, A&A, 296, 823
Van Dyke, M. 1982, An Album of Fluid Motion (Stanford: Parabolic)
Wood, D. O. S., & Churchwell, E. 1989, ApJS, 69, 831